

SPI-1-Dependent Host Range of Rabbitpox Virus and Complex Formation with Cathepsin G Is Associated with Serpin Motifs

KRISTIN B. MOON, PETER C. TURNER, AND RICHARD W. MOYER*

*Department of Molecular Genetics and Microbiology, University of Florida,
Gainesville, Florida 32610-0266*

Received 2 April 1999/Accepted 16 July 1999

Serpins are a superfamily of serine proteinase inhibitors which function to regulate a number of key biological processes including fibrinolysis, inflammation, and cell migration. Poxviruses are the only viruses known to encode functional serpins. While some poxvirus serpins regulate inflammation (myxoma virus SERP1 and cowpox virus [CPV] crmA/SPI-2) or apoptosis (myxoma virus SERP2 and CPV crmA/SPI-2), the function of other poxvirus serpins remains unknown. The rabbitpox virus (RPV) SPI-1 protein is 47% identical to crmA and shares all of the serpin structural motifs. However, no serpin-like activity has been demonstrated for SPI-1 to date. Earlier we showed that RPV with the SPI-1 gene deleted, unlike wild-type virus, fails to grow on A549 or PK15 cells (A. Ali, P. C. Turner, M. A. Brooks, and R. W. Moyer, *Virology* 202:306–314, 1994). Here we demonstrate that in the absence of a functional SPI-1 protein, infected nonpermissive cells which exhibit the morphological features of apoptosis fail to activate terminal caspases or cleave the death substrates PARP or lamin A. We show that SPI-1 forms a stable complex in vitro with cathepsin G, a member of the chymotrypsin family of serine proteinases, consistent with serpin activity. SPI-1 reactive-site loop (RSL) mutations of the critical P1 and P14 residues abolish this activity. Viruses containing the SPI-1 RSL P1 or P14 mutations also fail to grow on A549 or PK15 cells. These results suggest that the full virus host range depends on the serpin activity of SPI-1 and that in restrictive cells SPI-1 inhibits a proteinase with chymotrypsin-like activity and may function to inhibit a caspase-independent pathway of apoptosis.

Collectively, members of the serpin superfamily comprise single polypeptide chains of approximately 370 to 390 residues containing a conserved domain of three β -sheets and nine α -helices (14). A distorted α -helix extends from β -sheet A and contains the serpin reactive-site loop (RSL), which interacts directly with the target serine or cysteine proteinase. This RSL, which mimics the natural proteinase substrate, is located toward the C-terminal region of the protein. The RSL comprises amino acid residues designated P15 to P^{5'}, where proteolysis occurs at the scissile bond between residues P1 and P1' (12). Serpins function as inhibitors by forming long-lived complexes with their cognate proteinases, which are thought to persist as stable acyl-enzyme intermediates (15). Because the covalent complex between a serpin and serine proteinase is relatively stable, it remains intact following boiling and sodium dodecyl sulfate-polyacrylamide gel electrophoresis (SDS-PAGE). Interaction of the serpin RSL with a nontarget proteinase results in cleavage within the serpin reactive site without stable complex formation. There are noninhibitory serpins such as ovalbumin and angiotensinogen, which are devoid of any inhibitory activity and have evolved to fulfill roles other than proteinase inhibition (28).

In mammals, members of the serpin superfamily are involved in regulating inflammation, hormone activation, fibrinolysis, and cell migration (33). Serpins are remarkably specific for the proteinases they inhibit, and target enzyme specificity is largely due to the single amino acid found at the P1 residue of the serpin. The importance of the P1 residue and serpin specificity is best demonstrated in several human diseases, where specific mutations important for serpin activity result in the

inability of the serpin to inhibit its natural target proteinase (37). In the serpin mutant α_1 -antitrypsin Pittsburgh, the wild-type methionine P1 residue is mutated to arginine, resulting in the inability of the serpin to inhibit elastase. Instead, the mutant serpin gains the ability to inhibit the trypsin-like enzymes thrombin, kallikrein, factor Xa, and plasmin, resulting in a severe bleeding disorder (12, 26, 28).

Although poxviruses are the only virus family currently known to encode functional serpins, an open reading frame (ORF) with homology to the serpin superfamily but lacking a typical RSL has been found in gammaherpesvirus 68 (43). Members of the *Orthopoxvirus*, *Leporipoxvirus*, *Avipoxvirus*, and *Siipoxvirus* genera each encode serpins. One of the most extensively studied poxvirus serpins is the cytokine response modifier A, or crmA, from cowpox virus (CPV), known as B13R in vaccinia virus or SPI-2 in rabbitpox virus (RPV). Initial studies demonstrated that crmA prevents inflammation in vivo by inhibiting interleukin-1 β convertase (ICE; caspase 1) (30). crmA has also been shown to block apoptosis induced by a variety of different stimuli, including growth factor deprivation (11) and signalling through the Fas or type 1 tumor necrosis factor receptors (9, 17, 39). crmA is now known to inhibit some but not all members of the caspase family of cysteine proteinases, which regulate apoptosis, as well as granzyme B, a serine proteinase found in cytotoxic T-lymphocytes (CTLs) that mediates apoptosis during CTL-mediated death (23, 29, 32, 38, 50). Within the context of intact virus, crmA plays a role in preventing apoptosis during CPV infection of LLC-PK1 pig kidney cells (18, 31).

RPV SPI-1 has 47% identity to crmA. This fact, along with the conservation of SPI-1 in all orthopoxviruses including variola virus, the causative agent of smallpox, suggests that SPI-1 may play a role in viral pathogenesis. In conjunction with crmA/SPI-2, SPI-1 has been suggested to function to inhibit apoptosis induced by CTL-mediated killing, although the mecha-

* Corresponding author. Mailing address: Department of Molecular Genetics and Microbiology, College of Medicine, University of Florida, Box 100266, Gainesville, FL 32610-0266. Phone: (352) 392-7077. Fax: (352) 846-2042. E-mail: rmoyer@medmicro.med.ufl.edu.

nism of this inhibition is not known (19). RPV SPI-1 deletion mutants have a reduced host range and, unlike wild-type RPV (wtRPV), are unable to produce plaques on the restrictive (nonpermissive) A549 and PK15 cell lines (1). The inability of RPV SPI-1 deletion mutants to form plaques on restrictive cell lines reflects the absence of intracellular mature virus, intracellular enveloped virus, and extracellular enveloped virus from infected cells (3). This failure to produce progeny virus was proposed to result from the induction of apoptosis including chromatin condensation and nuclear invagination in restrictive cells infected with RPV SPI-1 mutants (3).

Although SPI-1 clearly plays a role in mediating viral host range, no biochemical activity has been attributed to SPI-1 to date. In this study, we demonstrate that RPVΔSPI-1 infection of restrictive cell lines results in the morphological features of apoptosis but without caspase 3 activation or cleavage of the death substrates poly(ADP-ribose) polymerase (PARP) or lamin A, suggesting that SPI-1 may act to inhibit a caspase-independent form of apoptosis. Using an in vitro system, we show that SPI-1 is able to form an SDS-stable complex with the serine proteinase cathepsin G, a member of the chymotrypsin family, indicating that SPI-1 is likely to be a functional proteinase inhibitor which utilizes the phenylalanine at position 322 as the P1 residue. Once formed, the complex is stable, with an estimated half-life of 23 h, properties consistent with proteinase inhibition. Furthermore, we are able to demonstrate that the ability of SPI-1 to function as a serpin is essential for virus growth in restrictive cell lines, suggesting that SPI-1 must inhibit a chymotrypsin-like proteinase to confer the full host range on RPV.

MATERIALS AND METHODS

Cells and viruses. A549, PK15, RK13, CV-1, and LLC-PK1 cells were obtained from the American Type Culture Collection. A549, PK15, RK13, and CV-1 cells were routinely grown in GIBCO-BRL minimum essential medium (MEM) with Earle's salts supplemented with 5% fetal bovine serum (FBS), 2 mM glutamine, 50 U of penicillin G per ml, 50 µg of streptomycin per ml, 1 mM sodium pyruvate, and 0.1 mM MEM nonessential amino acids (GIBCO). LLC-PK1 cells were grown in medium 199 (GIBCO) supplemented with 10% FBS, 2 mM glutamine, 50 U of penicillin G per ml, 50 µg of streptomycin per ml, 1 mM sodium pyruvate, and 0.1 mM MEM nonessential amino acids. wtRPV (Utrecht strain) was obtained from the American Type Culture Collection, and wtCPV (Brighton Red Strain) was obtained from David Pickup (Duke University). CPVΔcrmA (also known as CPVΔSPI-2) has been described previously (1). Cells and viruses were grown at 37°C. Virus stocks were routinely grown on CV-1 cells, which were also used for determination of virus titers.

Construction of recombinant viruses. The shuttle vector pKMSP1-1 was constructed to replace the wt SPI-1 gene with the selectable marker *eco-gpt* or each of the three SPI-1 site-directed mutant genes (discussed below) in the RPV genome. Briefly, the 235 bp directly upstream of the SPI-1 ORF (SPI-1 left flank) were amplified from wtRPV genomic DNA by PCR with primers RM 536 (5'GCTCTAGACGATTGATTATCATTACCC 3') and RM 537 (5'CGGAATTCATGGTATAAACAAATAGACTTT TAT 3') (Fig. 1A), which introduced an *Xba*I site onto the 5' end and *Nco*I and *Eco*RI sites onto the 3' end of the flank, respectively. The SPI-1 left flank was digested with *Xba*I and *Eco*RI and cloned into pBluescript KS(+). The 522 bp directly downstream of the SPI-1 ORF (SPI-1 right flank) were amplified from wtRPV genomic DNA by PCR with primers RM 540 (5' CGGAATTCCGATCATATAAACAAATAGACTTT TAT 3') and RM 539 (5' GCGTCGACTCTATAGAACACCTAGAATA 3'), which introduced *Eco*RI and *Bam*H I sites onto the 5' end and a *Sal*I site onto the 3' end of the flank, respectively. The SPI-1 right flank was digested with *Eco*RI and *Sal*I and cloned into pBluescript KS(+) containing the SPI-1 left flank, to create pKMSP1-1 (Fig. 1B). To delete the SPI-1 gene from RPV, a 2,081-bp fragment containing the *Escherichia coli* *gpt* gene downstream of the vaccinia virus *P*_{7.5} promoter was cloned between the SPI-1 left and right flanks into the *Eco*RI site in pKMSP1-1 (pKMSP1-1-gpt). To create the wt reconstructed virus as well as virus recombinants containing SPI-1 site-directed mutations, the wt SPI-1 and each of the three SPI-1 site-directed mutant genes (discussed below) were excised from pAlter-Ex1 by digestion with *Nco*I and *Bam*H I and subcloned into pKMSP1-1 (pKMSP1-1 wt, pKMSP1-1 N321A/F322A/S323A, pKMSP1-1 F322A, and pKMSP1-1 T309R).

To create recombinant virus, semiconfluent (80%) CV-1 cells grown in 35-mm dishes were infected with virus at a multiplicity of infection (MOI) of 0.05 and virus was adsorbed for 2 h at 37°C. The inoculum was removed, and the cells

were washed twice with GIBCO MEM without serum. A 1.5-ml volume of medium without serum was added to the cells, followed by 5 to 10 µg of the appropriate plasmid conjugated with Lipofectin in a 100-µl volume. At 24 h postinfection, 1.5 ml of GIBCO MEM supplemented with 5% FBS was added to the cells, which were incubated for another 24 h at 37°C. Transfected cells were harvested at 48 h postinfection. Virus recombinants containing *eco-gpt* (RPVΔSPI-1) were selected by their resistance to mycophenolic acid (2, 10). Viral recombinants containing the wt or mutant SPI-1 genes in place of *eco-gpt* were selected following plaque hybridization with a ³²P-labeled randomly primed probe specific for the SPI-1 gene. All viral recombinants were purified through three rounds of plaque purification. The desired genotype of the recombinant viruses was confirmed by PCR and immunoblot analysis with a SPI-1-specific antibody.

Preparation of infected cell extracts for PARP and lamin A cleavage assays. Semiconfluent (80%) monolayers of either A549 or LLC-PK1 cells in 60-mm dishes were either mock infected or infected with wtRPV or RPVΔSPI-1 (A549 cells) or with wtCPV or CPVΔcrmA (LLC-PK1 cells) at an MOI of 10. Virus was adsorbed to cells for 2 h at 37°C, medium was added, and the infection was allowed to proceed for 14 h. The cells were harvested by scraping into the medium and were pelleted for 5 min at 200 × g. Cells were washed once with phosphate-buffered saline (pH 7.4), pelleted, washed once in ice-cold extract preparation buffer (EBP [50 mM piperazine-N,N'-bis(2-ethanesulfonic acid) (PIPES; pH 7.0), 50 mM KCl, 5 mM EGTA, 2 mM MgCl₂, 1 mM dithiothreitol (DTT), 20 µM cytochalasin B], pelleted, and resuspended in 100 to 200 µl of cold EBP containing the proteinase inhibitors phenylmethylsulfonyl fluoride (PMSF; 0.2 mM) and CLAP (containing chymostatin [20 µg/ml], leupeptin [5 µg/ml], antipain [20 µg/ml], and pepstatin A [5 µg/ml]). The cells were lysed by four cycles of freezing and thawing, and the lysates were subjected to centrifugation at 10,000 × g for 15 min. The supernatant cytoplasmic extract was either used immediately or stored at -80°C. The protein concentration was determined by the Bradford assay.

In vitro expression of PARP and human lamin A and cleavage assay. Human lamin A was expressed in an in vitro system as described previously (18). A cDNA clone of human PARP (kindly provided by Alexander Burkle, German Cancer Research Center, Heidelberg, Germany) was cloned with *Sma*I into the plasmid pGEM 3ZF(-), oriented such that PARP could be expressed from the *P*_{T7} promoter. ³⁵S-labeled PARP was synthesized with the T7 Quick TNT system (Promega Corp.) as specified by the manufacturer. The presence of lamin A- or PARP-cleaving activity in cell extracts was determined by adding 2 µl of ³⁵S-labeled lamin A or PARP from a 50-µl transcription-translation reaction mixture to 15 µg of extract from either mock-infected or infected cell extracts followed by a 90-min incubation at 37°C. Proteins were resolved on SDS-10% polyacrylamide gels, the radioactive signal was enhanced with Amplify (Amersham), and the proteins were visualized by autoradiography.

Preparation of infected-cell extracts and caspase 3 assay. Cells grown in 60-mm dishes were mock infected with medium alone or infected with wtRPV or RPVΔSPI-1 (A549 cells) or with wtCPV or CPVΔcrmA (LLC-PK1 cells) at an MOI of 10. Virus was adsorbed for 2 h at 37°C, medium was added, and the infection was allowed to proceed for 14 h at 37°C. Cells were harvested by being scraped into the medium and were pelleted for 5 min at 200 × g. The cells were washed once in phosphate-buffered saline (pH 7.4), pelleted, and then resuspended in 100 µl of caspase extract buffer (10 mM HEPES [pH 7.5], 2 mM EDTA, 0.1% CHAPS, 1 mM DTT). The cells were subjected to four cycles of freezing and thawing, followed by centrifugation at 10,000 × g for 15 min. Supernatant cytoplasmic extract was used immediately or stored at -80°C. The protein concentration was determined by the Bradford assay. A 2.5-µg portion of cell extract was brought to 50 µl with caspase extract buffer in a well of a 96-well microplate. The reaction was started by adding 150 µl of caspase extract buffer containing 0.1 mM fluorogenic caspase 3 substrate Ac-DEVD-AMC (diluted 1:1,000 from a 10 mM stock prepared in dimethyl sulfoxide). Substrate cleavage indicative of caspase 3-like activity was followed by fluorometry, with an excitation wavelength of 360 nm and an emission wavelength of 465 nm using a Tecan Microplate Reader.

In vitro expression of wt SPI-1, His-tagged SPI-1 and SPI-1 site-directed mutants. The wt and site-directed mutant SPI-1 genes were cloned into the vector pAlter-Ex1 (Promega Corp.) by using *Nco*I and *Bam*H I, oriented such that the genes could be expressed from the *P*_{T7} promoter. SPI-1 was likewise cloned into the vector pTM1-His by using *Nco*I and *Bam*H I oriented such that the gene could be expressed from the *P*_{T7} promoter and allowing the incorporation of a decahistidine tag onto the N terminus of the protein. In vitro expression of ³⁵S-labeled wt SPI-1, His-tagged SPI-1, and each of the three SPI-1 site-directed mutants was performed with the TNT T7 Quick Coupled Transcription/Translation system (Promega Corp.) as specified by the manufacturer.

SDS-PAGE analysis of SPI-1 activity. Samples (1 µl) of ³⁵S-labeled wt SPI-1 or SPI-1 RSL mutants expressed in vitro in the TNT system were incubated with various amounts of the proteinases human pancreas chymotrypsin, human neutrophil cathepsin G (both purchased from Athens Research and Technology, Inc., Athens, Ga.), or recombinant mast cell chymase (generous gift from Norman Schechter, University of Pennsylvania). The reactions were performed for 90 min at 37°C in a total volume of 10 µl containing the appropriate reaction buffer (100 mM Tris-HCl [pH 8.0]-10 mM CaCl₂ was used with the proteinases chymotrypsin and cathepsin G; 1.5 M NaCl-0.5 M Tris-HCl [pH 8.0]-9% di-

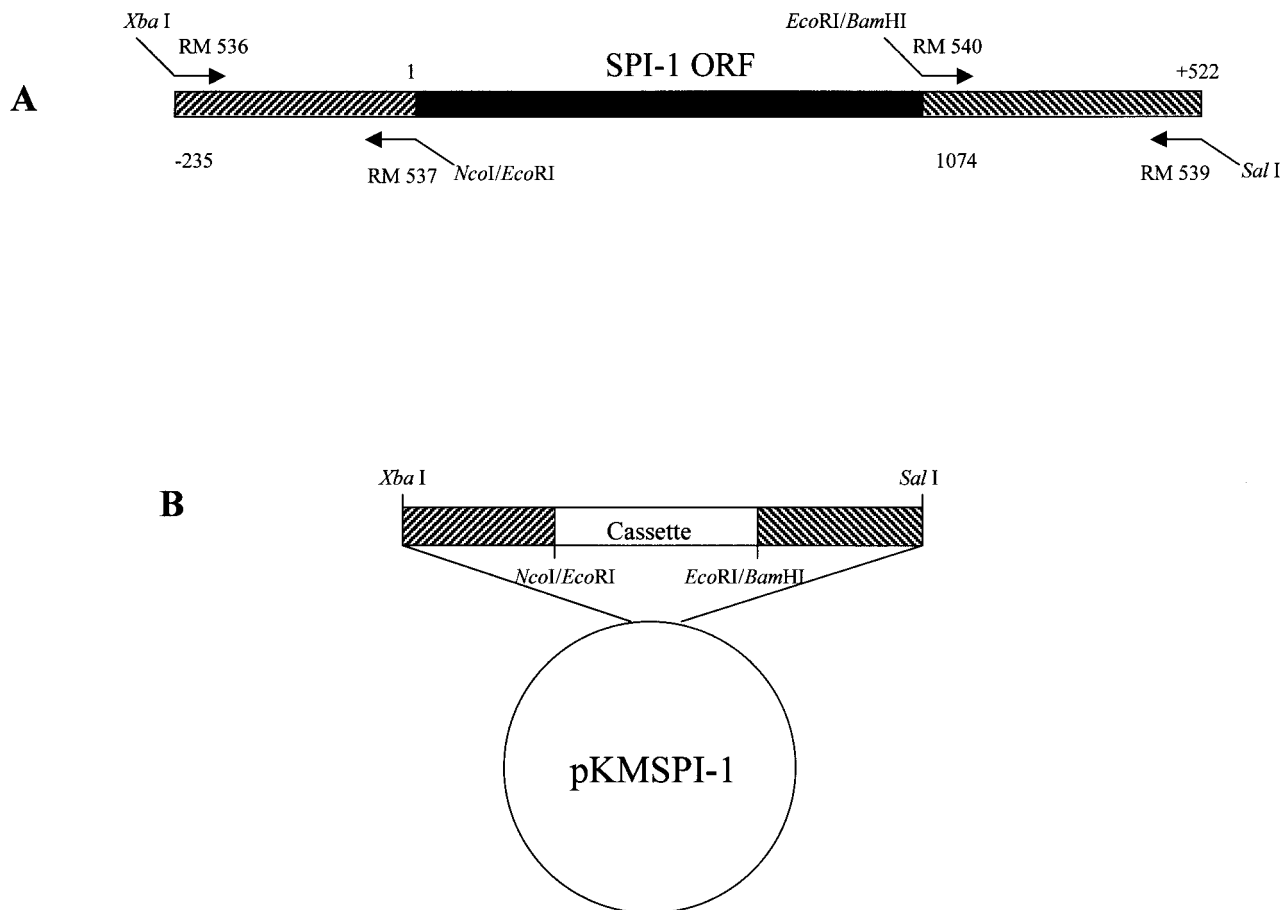


FIG. 1. Construction of the SPI-1 shuttle vector. (A) Source of the primers used to amplify the left and right flanks of SPI-1 for construction of the shuttle vector pKMSPI-1. This plasmid was used to replace the wt SPI-1 gene with the selectable marker *eco-gpt* or each of the three SPI-1 site-directed mutant genes in the RPV genome. The SPI-1 ORF beginning with nucleotide 1 and ending with nucleotide 1074 is designated by a black box. The left flanking sequence of the SPI-1 gene begins at nucleotide -235 and extends to nucleotide 1 of the SPI-1 ORF. The right flanking sequence of SPI-1 begins at the first nucleotide following the SPI-1 ORF and extends to nucleotide +522. SPI-1 left and right flanks are designated by hatched boxes. (B) Schematic of the SPI-1 shuttle vector, pKMSPI-1. A removable cassette containing either the *E. coli* *gpt* gene driven by the vaccinia virus P_{7.5} promoter, the wt SPI-1 gene, or each of the SPI-1 site-directed mutant genes was cloned between the left and right flanks of SPI-1. The locations of the relevant restriction sites are shown.

methyl sulfoxide was used with mast cell chymase). The reactions were stopped by the addition of SDS sample buffer containing 100 mM DTT and boiling for 5 min. Proteins were separated on SDS-10% polyacrylamide gels, ^{35}S -labeled proteins were enhanced with Amplify (Amersham), and the proteins were visualized by autoradiography.

His-tagged protein purification. Samples (5 µl) of ^{35}S -labeled His-tagged SPI-1 expressed in the TNT system were incubated with buffer alone or with 200 nM chymotrypsin G or chymotrypsin in a total volume of 20 µl for 15 min at 37°C. The reaction products were then added to 30 µl of His-Bind resin (Novagen) which had been charged with 50 mM NiSO₄ for 5 min. The mixtures were incubated at 4°C for 2 h with constant agitation. The resin was washed with 500 µl of MCAC-50 (20 mM Tris-HCl [pH 7.9], 0.5 M NaCl, 10% glycerol, 1 mM PMSF, 50 mM imidazole) and then with 500 µl of MCAC-100 (20 mM Tris-HCl [pH 7.9], 0.5 M NaCl, 10% glycerol, 1 mM PMSF, 100 mM imidazole) to remove any unbound proteins. His-tagged proteins were removed from the resin by the addition of 2× SDS-PAGE sample buffer followed by boiling for 5 min. The proteins were separated on SDS-10% polyacrylamide gels, and radiolabeled proteins were visualized by autoradiography.

Complex formation assay. Samples (10 µl) of ³⁵S-labeled SPI-1 prepared in the TNT system were incubated with buffer alone or with 200 nM cathepsin G in a total volume of 100 µl at 37°C. Portions were removed at intervals, and the reactions were quenched by the addition of 2× SDS sample buffer containing 100 mM DTT and boiled for 5 min, and the proteins were separated on SDS-10% polyacrylamide gels. Radiolabeled proteins were enhanced with Amplify, and the proteins were visualized by autoradiography.

Antichymotrypsin competition assay. Human plasma α_1 -antichymotrypsin was purchased from Athens Research and Technology, Inc. A 1- μ l volume of 35 S-labeled wt SPI-1 expressed in the TNT system was reacted with a constant amount of cathepsin G previously shown to yield complex formation (200 nM) in

the presence of increasing amounts of antichymotrypsin. Reactions were performed in a total volume of 10 μ l containing reaction buffer (100 mM Tris-HCl [pH 8.0], 10 mM CaCl₂) for 90 min at 37°C. The reactions were quenched by the addition of SDS sample buffer containing 100 mM DTT and boiling for 5 min, and the products were analyzed by electrophoresis on SDS-10% polyacrylamide gels. ³⁵S-labeled proteins were enhanced with Amplify, and the proteins were visualized by autoradiography.

Time course of SPI-1–cathepsin G complex stability. A 15- μ l volume of 35 S-labeled wt SPI-1 expressed in the TNT system was incubated with 200 nM cathepsin G in a total volume of 150 μ l of reaction buffer for 60 min at 37°C. A 10-fold molar excess of antichymotrypsin (2 μ M) was added to the reaction mixture, which was then incubated for up to 24 h at 37°C. Samples were removed at various times, and reactions were quenched by the addition of SDS sample buffer containing 100 mM DTT and boiled for 5 min. Proteins were separated on an SDS–10% polyacrylamide gel, 35 S-labeled proteins were enhanced with Amplify, and the proteins were visualized by autoradiography. High-molecular-weight bands representing the SPI-1–cathepsin G complex were quantified with a Molecular Dynamics, Inc., model 400S PhosphorImager.

Site-directed mutagenesis of SPI-1. Site-directed mutagenesis of the SPI-1 reactive site was performed with the Altered Sites mutagenesis system (Promega Corp.) as specified by the manufacturer. The RPV SPI-1 open reading frame was first subcloned into the pAlter-Ex1 vector *Nco*I and *Bam*HI sites. The 5'-phosphorylated oligonucleotide (RM 538) (5'p-ACAGGAGTATTATGACTACA GCTGCGATGGTATATCGTACGAAG-3') was used to change the predicted P2, P1, and P1' residues at positions 321, 322, and 323 from asparagine, phenylalanine, and serine to alanine, alanine, and alanine (N321A/F322A/S323A). The 5'-phosphorylated oligonucleotides GM14 (5'p-GGAGTATTATGACTAAC GCGTCGATGGTATATCGTACG-3') and RM 543 (5'p-GATGTTAACATGAG GAGTATCGCGAACGATCGGCCGT-3') were likewise used to change the

predicted P1 residue at position 322 from phenylalanine to alanine (F322A) and the P14 residue at position 309 from threonine to arginine (T309R). The sequence of the site-directed mutants was confirmed by sequencing.

Virus plaque assay. RK13, A549, and PK15 cell monolayers grown in 60-mm dishes were infected with approximately 100 PFU of wtRPV, RPVΔSPI-1, RPV SPI-1 N321A/F322A/S323A, RPV SPI-1 F322A, or RPV SPI-1 T309R in GIBCO MEM without serum. After 2 h of incubation at 37°C, the virus inoculum was removed and the infected cells were overlaid with a 1:1 mixture of 2× GIBCO MEM and 1.2% agarose. At 72 h postinfection, the agarose overlays were removed and the infected cell monolayers were stained with crystal violet.

DAPI staining of infected cells. A549 cells were grown in LabTek eight-well chamber slides (Nunc) to 60% confluence and infected with virus at an MOI of 10 in 100 µl of GIBCO MEM without serum. Virus was adsorbed for 2 h at 37°C. After removal of the inoculum, the cells were washed with 300 µl of medium without serum. The cells were processed for 4',6-diamidino-2-phenylindole (DAPI) staining at 18 h postinfection as described previously (18). Fluorescent cells were photographed with Fuji 400 ASA film.

RESULTS

Caspase 3 activity and cleavage of death-associated substrates in infected-cell extracts. Our laboratory has previously shown that infection of nonpermissive cells with RPV SPI-1 mutants results in the morphological features of apoptosis, including chromatin condensation and nuclear invagination (3). Caspases are a family of cysteine proteinases which cleave specifically after aspartic acid residues and are key executioners in the apoptotic cascade (24). Activation of the executioner caspases, which include caspases 3, 6, and 7, is responsible for cleavage of the death substrates, including the DNA repair enzyme PARP and components of the nuclear lamina (lamins A and B/C) (24). We wished to determine whether, in addition to the morphological features of apoptosis in A549 cells infected with RPV SPI-1 mutants, the cells displayed the expected accompanying biochemical changes associated with apoptosis, such as caspase activation and cleavage of death substrates.

An RPV SPI-1 deletion mutant (RPVΔSPI-1), in which the entire SPI-1 ORF was replaced with the gene for the selectable marker encoded by the *gpt* gene of *E. coli* under the control of the vaccinia virus P_{7.5} promoter, was created (Fig. 1). The absence of SPI-1 was confirmed by PCR and Western blot analysis (data not shown). To ensure that no unintended mutations had been introduced into the virus during the construction of RPVΔSPI-1, wt virus was reconstructed by replacing the *eco-gpt* gene with the wt SPI-1 gene. The reintroduction of the SPI-1 gene into the wt reconstructed virus was confirmed by PCR and Western blot analysis (data not shown). The reconstructed virus was then assayed for the ability to form plaques on restrictive and nonrestrictive cell lines and was found to be indistinguishable from wtRPV (data not shown).

A549 cells were mock infected or infected with wtRPV or RPVΔSPI-1 at an MOI of 10, and infected-cell extracts were prepared at 14 h postinfection. Extracts were also made from LLC-PK1 cells which were mock infected or infected with wtCPV or CPVΔcrmA. Previous studies have shown that LLC-PK1 cells infected with CPVΔcrmA but not wtCPV undergo apoptosis accompanied by the expected cleavage of PARP and lamin A (18). Extracts were incubated with ³⁵S-labeled PARP (Fig. 2A) or lamin A (Fig. 2B) for 90 min at 37°C, and the products were analyzed following SDS-PAGE and autoradiography. Extracts prepared from LLC-PK1 cells infected with CPVΔcrmA but not wtCPV cleave PARP (116 kDa) to the expected 85- and 30-kDa fragments (Fig. 2A, lane 3). Likewise, extracts prepared from LLC-PK1 cells infected with CPVΔcrmA cleave lamin A from its native form to a 30-kDa product (Fig. 2B, lane 3), again consistent with previous studies (18). In contrast, no PARP or lamin A cleavage was seen when these substrates were incubated with extracts prepared from A549

cells infected with RPVΔSPI-1. Infected-cell extracts were also assayed for the induction of caspase 3-like activity by using the fluorogenic substrate Ac-DEVD-AMC (Fig. 2C) as a more direct assay for caspase activation. Only extracts prepared from LLC-PK1 cells infected with CPVΔcrmA induced caspase 3-like activity, as determined by substrate cleavage, whereas extracts from A549 cells infected with wtRPV or RPVΔSPI-1 did not. Thus, while A549 cells infected with RPV SPI-1 mutants undergo the morphological changes associated with apoptosis, these changes occur in the absence of the normally accompanying activation of caspases and cleavage of the death substrates PARP and lamin A. These results suggest that during infection, SPI-1 may be involved in regulating a caspase-independent form of apoptosis.

Ability of SPI-1 to form complexes with serine proteinases. Although RPV requires SPI-1 for growth on A549 and PK15 cells (1), SPI-1 has never been demonstrated to act as a proteinase inhibitor either in vitro or in vivo. The amino acid sequence of the SPI-1 RSL was compared to the RSLs of cellular inhibitory and noninhibitory serpins and viral serpins (Fig. 3). SPI-1, like most inhibitory serpins, contains a threonine at the P14 position (residue 309), in contrast to the charged arginine residue found at the P14 position in the noninhibitory serpins ovalbumin and angiotensinogen. The presence of arginine at the hinge region of noninhibitory serpins is thought to prevent reactive-site loop insertion due to steric hindrance. The presence of an uncharged amino acid at the hinge region of SPI-1 suggests that reactive-site loop insertion into the serpin backbone could occur following association with its target proteinase, allowing the formation of a stable inhibitory complex. Based on alignment with other serpins, the predicted P1 residue of SPI-1 is the phenylalanine located at position 322. Therefore, we reasoned that SPI-1 may be active against members of the chymotrypsin family of serine proteinases.

As an initial screen for potential target proteinases of SPI-1, we exploited the ability of serpins to form an SDS-stable complex with proteinases which they inhibit (28). This assay takes advantage of ³⁵S-labeled SPI-1 prepared in an in vitro coupled transcription-translation system (TNT; Promega Corp.), which is then assayed for complex formation against a panel of suspected proteinase targets. In the specific case of SPI-1, we probed members of the chymotrypsin family (Fig. 4A), including cathepsin G, chymotrypsin, and mast cell chymase. Radiolabeled SPI-1, when incubated with chymotrypsin and mast cell chymase, was cleaved to produce a 40-kDa species which migrated slightly faster than uncleaved SPI-1 when analyzed on an SDS-10% polyacrylamide gel (Fig. 4A, lanes 4 to 8). Likewise, SPI-1 that was reacted with cathepsin D, thrombin, and elastase yielded a similar 40-kDa product (data not shown). When radiolabeled SPI-1 was exposed to cathepsin G, some cleavage was also observed, but in addition, higher-molecular-mass protein products were generated (lanes 2 and 3). The size of the novel, higher-molecular-mass proteins (approximately 65 to 70 kDa) is consistent with the expected size of an SDS-stable complex between SPI-1 (~45 kDa) and cathepsin G (~25 kDa). Thus, while SPI-1 is solely a substrate for cathepsin D, mast cell chymase, chymotrypsin, thrombin, and elastase, it forms an SDS-stable, high-molecular-mass complex with cathepsin G, indicative of inhibition.

Incubation of SPI-1 with all of the enzymes tested resulted in the formation of a 40-kDa cleavage product (Fig. 4A, dashed arrow). A 40-kDa product is consistent with cleavage within the SPI-1 RSL, followed by release of a ~4-kDa product representing the C terminus of the protein. To test this hypothesis, we generated ³⁵S-labeled SPI-1 containing an oligohistidine

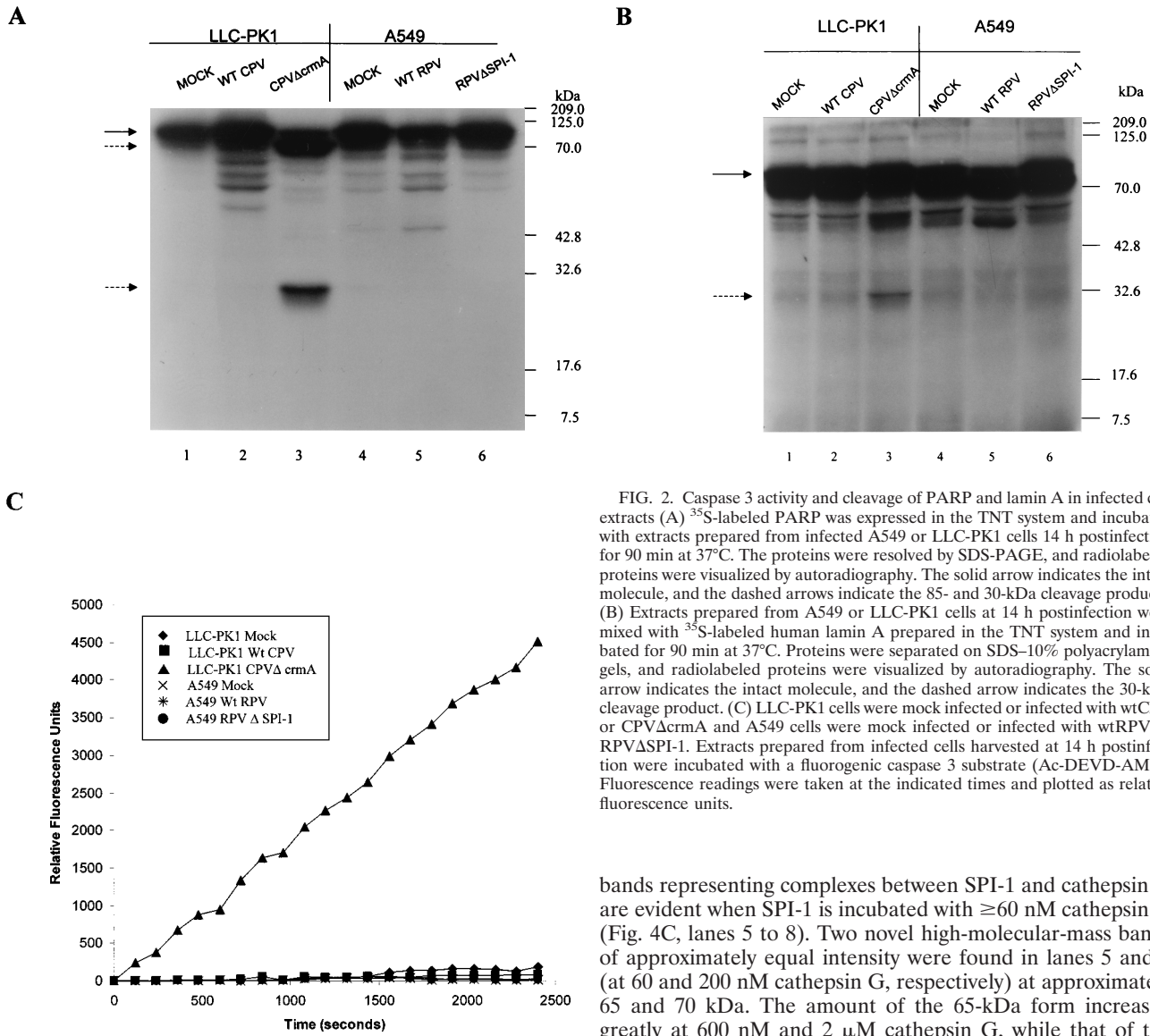


FIG. 2. Caspase 3 activity and cleavage of PARP and lamin A in infected cell extracts (A) ³⁵S-labeled PARP was expressed in the TNT system and incubated with extracts prepared from infected A549 or LLC-PK1 cells 14 h postinfection for 90 min at 37°C. The proteins were resolved by SDS-PAGE, and radiolabeled proteins were visualized by autoradiography. The solid arrow indicates the intact molecule, and the dashed arrows indicate the 85- and 30-kDa cleavage products. (B) Extracts prepared from A549 or LLC-PK1 cells at 14 h postinfection were mixed with ³⁵S-labeled human lamin A prepared in the TNT system and incubated for 90 min at 37°C. Proteins were separated on SDS-10% polyacrylamide gels, and radiolabeled proteins were visualized by autoradiography. The solid arrow indicates the intact molecule, and the dashed arrow indicates the 30-kDa cleavage product. (C) LLC-PK1 cells were mock infected or infected with wtCPV or RPVΔSPI-1. Extracts prepared from infected cells harvested at 14 h postinfection were incubated with a fluorogenic caspase 3 substrate (Ac-DEVD-AMC). Fluorescence readings were taken at the indicated times and plotted as relative fluorescence units.

tag at the N terminus by using the TNT system. The protein was incubated alone or with the enzyme cathepsin G or chymotrypsin (Fig. 4B) for 15 min to allow cleavage. His-tagged proteins, purified by binding to His-Bind resin, were analyzed following SDS-PAGE and autoradiography. His-tagged SPI-1 migrates as a ~49-kDa band on the gel (Fig. 4B, lane 1). A high-molecular-mass band representing a complex between His-tagged SPI-1 and cathepsin G was seen (lane 2). Following incubation with cathepsin G (lane 2) or chymotrypsin (lane 3), a His-tagged product of ~45 kDa was visible. The fact that the smaller (45-kDa) products retained their N-terminal His tags and were visible following purification over the nickel column is consistent with cleavage occurring at the C termini of the proteins within the SPI-1 RSL.

The above experiments demonstrate that SPI-1 is able to form an SDS-stable complex with cathepsin G. To examine the interaction between the two proteins over a range of enzyme concentrations, SPI-1 prepared in the TNT system was incubated with threefold-increasing concentrations of cathepsin G ranging from 2 nM to 2 μM (Fig. 4C). High-molecular-mass

bands representing complexes between SPI-1 and cathepsin G are evident when SPI-1 is incubated with ≥60 nM cathepsin G (Fig. 4C, lanes 5 to 8). Two novel high-molecular-mass bands of approximately equal intensity were found in lanes 5 and 6 (at 60 and 200 nM cathepsin G, respectively) at approximately 65 and 70 kDa. The amount of the 65-kDa form increased greatly at 600 nM and 2 μM cathepsin G, while that of the 70-kDa form decreased (lanes 7 and 8, respectively), indicating that the 65-kDa form is the final complex.

To test the hypothesis that the proportion of the 65-kDa form of the complex increases with time, SPI-1 was incubated with cathepsin G (200 nM) at a concentration known to yield complex formation and samples were removed at various times after incubation at 37°C (Fig. 4D). Both the 70- and 65-kDa bands first appeared after a 5-min incubation at 37°C (lane 4). Over time, the intensity of the 70-kDa band appeared to decrease while the intensity of the 65-kDa band appeared to increase (lanes 5 to 8). These data suggest that the 70-kDa band is formed first and then decays to form the 65-kDa band. This decay is probably the result of enzymatic degradation of the 70-kDa SPI-1–cathepsin G complex to the smaller (65-kDa) form by excess unreacted cathepsin G. A similar observation has been reported for interactions between the inhibitory serpin antichymotrypsin and cathepsin G (27) or chymotrypsin (35). In each of these studies, it was determined that to obtain a stable irreversible complex between the serpin and cathepsin G or chymotrypsin, a high-molecular-weight intermediate form of the complex must be cleaved by free enzyme to produce a final lower-molecular-weight form (27, 35).

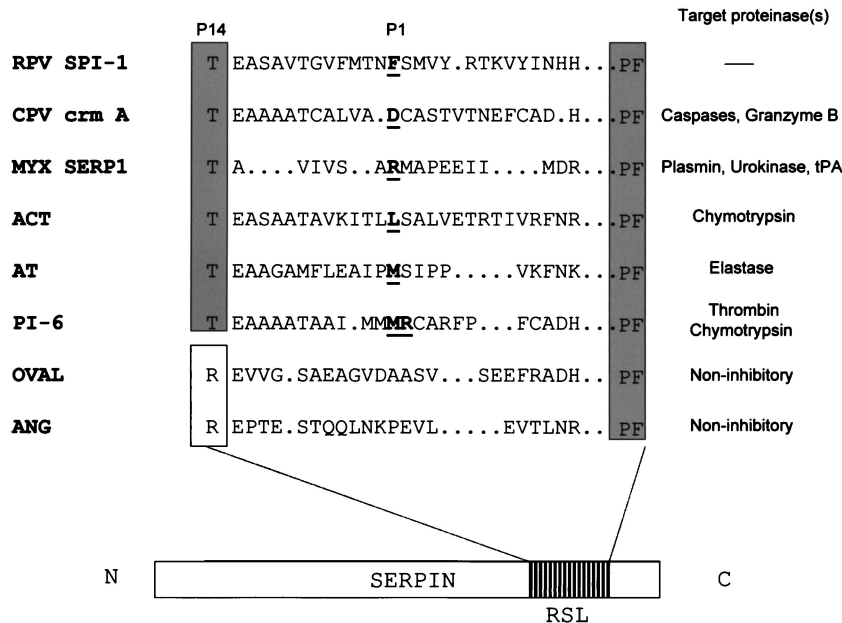


FIG. 3. Comparison of the SPI-1 RSL with inhibitory and noninhibitory serpins. A diagram of a typical serpin showing the location of the RSL is shown at the bottom of the figure. An alignment of the reactive site loops of selected cellular or viral serpins is shown, along with the proteinase(s) targeted by each serpin. Sequences begin with the P14 residue of each serpin and terminate with the conserved PF residues at the end of the motif. P1 residues are shown in bold and underlined. Serpin PI-6 is known to have two P1 residues. The predicted P1 amino acid of SPI-1 is also shown. Critical amino acid motif regions among serpins are boxed. Abbreviations: MYX, myxoma virus; ACT, antichymotrypsin; AT, antitrypsin; OVAL, ovalbumin; ANG, Angiotensinogen; tPA, tissue plasminogen activator. Of the serpins shown, only OVAL and ANG are noninhibitory serpins.

Complex formation between SPI-1 and cathepsin G is inhibited by the serpin antichymotrypsin. The inhibitory mechanism of serpins depends on nucleophilic attack on the serpin P1-P1' scissile bond by the catalytic serine of the target proteinase. To prove that complex formation between cathepsin G and SPI-1 is dependent on the presence of active cathepsin G, radiolabeled SPI-1 and cathepsin G were incubated in the presence of the serpin antichymotrypsin, a competing natural inhibitor of cathepsin G (Fig. 5). Radiolabeled SPI-1 (prepared in the TNT system as described above) was incubated alone (Fig. 5, lane 1) or with cathepsin G (200 nM) under conditions demonstrated to yield complex formation as shown in Fig. 4C. The reactions were performed in the absence (Fig. 5, lane 2) or presence (lanes 3 to 9) of increasing amounts of antichymotrypsin. The formation of complexes between cathepsin G and radiolabeled SPI-1 was again reflected by the presence of 65- and 70-kDa protein bands following separation of the reactants by SDS-PAGE (lanes 2 to 4). Radiolabeled complex formation was inhibited in the presence of 200 nM antichymotrypsin (lane 5) as expected, consistent with the ability of antichymotrypsin to compete with SPI-1 for complex formation with cathepsin G at a 1:1 molar ratio. SPI-1 does not form a complex with cathepsin G in the presence of higher concentrations of antichymotrypsin (600 nM [lane 6] to 200 μ M [lane 9]). These results indicate that SPI-1 and antichymotrypsin compete for the active site of cathepsin G and that active cathepsin G is required for complex formation, consistent with SPI-1 acting as an inhibitory serpin.

Stability of the SPI-1–cathepsin G complex. Inhibitory complexes between serpins and their target proteinases are stable for hours to even days before hydrolyzing (28). We asked whether the complex between SPI-1 and cathepsin G is stable, as would be expected following reaction of an inhibitory serpin with a target proteinase (Fig. 6). 35 S-labeled SPI-1 expressed in the TNT system (Fig. 6, lane 1) was incubated with 200 nM

cathepsin G for 60 min at 37°C to allow complex formation. A sample was removed after the 1-h preincubation period to ensure that complex formation had occurred (lane 2). Then a 10-fold molar excess of antichymotrypsin (2 μ M) was added to the reaction mixture to inactivate any remaining cathepsin G and prevent further reaction of cathepsin G with SPI-1. The reaction mixture was further incubated for up to 24 h at 37°C, and samples were removed for analysis at 1, 2, 3, 4, 5, 6, 7, 8, 9, and 24 h after the addition of antichymotrypsin and analyzed by SDS-PAGE (Fig. 6, lanes 3 to 12). Complex formation has occurred following the initial preincubation of SPI-1 and cathepsin G (lane 2). The complex remained visible throughout the experiment, decreasing in intensity by 24 h after the addition of antichymotrypsin. High-molecular-mass bands representing complexes between SPI-1 and cathepsin G in lanes 3 to 12 were measured with a PhosphorImager. PhosphorImager measurements from three separate experiments were averaged and expressed graphically as log units versus time (inset). Based on the graph, the half-life of the complex between SPI-1 and cathepsin G was estimated to be 22.5 h. The relatively long half-life of complexes formed between SPI-1 and cathepsin G is consistent with a model whereby SPI-1 functions as an inhibitory serpin active against cathepsin G.

Role of the RSL of SPI-1 in complex formation with cathepsin G. To determine whether the predicted SPI-1 reactive-site loop region is required for complex formation with cathepsin G, site-directed mutagenesis of the SPI-1 RSL was performed. The first mutant, N321A/F322A/S323A, was designed to alter not only the predicted P1 residue of the RSL but the adjacent P2 and P1' amino acids as well (Fig. 3). 35 S-labeled wt and mutant proteins were prepared in the TNT system and added to cathepsin G (Fig. 7A and B). Mutant SPI-1 protein was cleaved within or near the RSL, as indicated by the presence of a ~40-kDa band that migrates slightly faster than the uncleaved protein (Fig. 7B). However, no SDS-stable complex

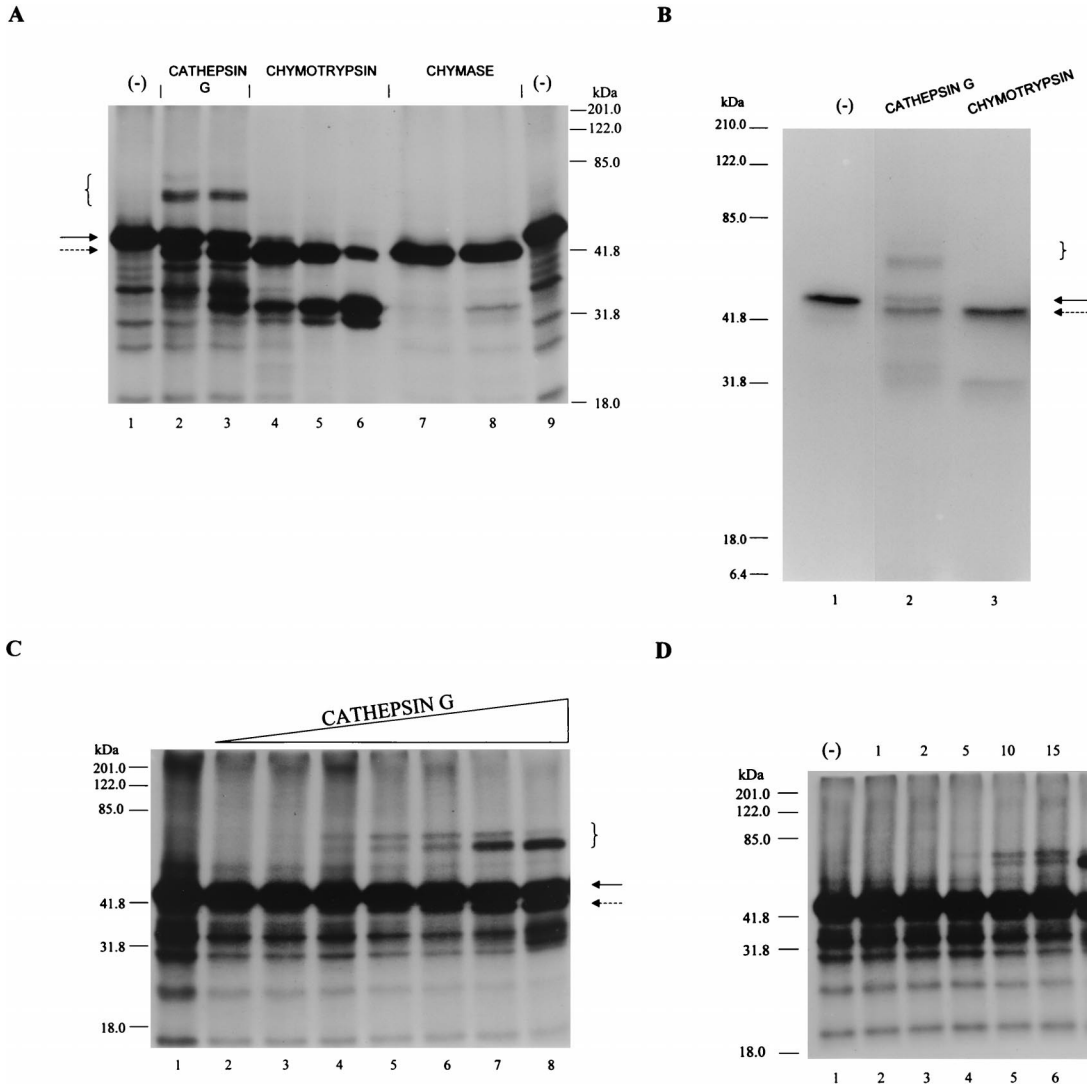


FIG. 4. Target proteinase specificity of SPI-1. (A) ^{35}S -labeled SPI-1 (prepared by in vitro transcription and translation with the TNT system) was incubated with buffer alone (lanes 1 and 9), 200 nM cathepsin G (lane 2), 600 nM cathepsin G (lane 3), 60 nM chymotrypsin (lane 4), 200 nM chymotrypsin (lane 5), 600 nM chymotrypsin (lane 6), 200 nM mast cell chymase (lane 7), or 600 nM mast cell chymase (lane 8). Reaction mixtures were incubated at 37°C for 90 min. Radiolabeled proteins were visualized following SDS-PAGE and autoradiography. (B) ^{35}S -labeled His-tagged SPI-1 prepared in the TNT system was incubated with buffer alone (lane 1) or with 200 nM cathepsin G (lane 2) or chymotrypsin (lane 3) for 15 min at 37°C. His-tagged products were purified by binding to His-Bind resin, and purified products were detected following SDS-PAGE and autoradiography. (C) ^{35}S -labeled SPI-1 (1 μl of a 50- μl TNT reaction mixture) was incubated with buffer alone (lane 1) or with threefold-increasing concentrations of cathepsin G ranging from 2 nM (lane 2) to 2 μM (lane 8) for 90 min at 37°C. (D) ^{35}S -labeled SPI-1 (1 μl of a 50- μl TNT reaction mixture) was incubated with buffer alone (lane 1) or with 200 nM cathepsin G for 1 (lane 2), 2 (lane 3), 5 (lane 4), 10 (lane 5), 15 (lane 6), 30 (lane 7), or 60 (lane 8) min at 37°C. Proteins were resolved on SDS-10% polyacrylamide gels, and radiolabeled proteins were visualized by autoradiography. Uncleaved SPI-1 and SPI-1 cleaved within the RSL are indicated by solid and dashed arrows, respectively. High-molecular-mass bands indicating the formation of SDS-stable complexes between SPI-1 and cathepsin G are designated by brackets.

was visible between the mutant and cathepsin G. Thus, it appears that the putative P1 residue of SPI-1 resides within the three mutated residues, probably at position 322.

To test this prediction, a second mutant, F322A, was made, with only the phenylalanine at the predicted P1 position (amino acid 322) changed to alanine. ^{35}S -labeled F322A synthesized in the TNT system was incubated with increasing concentrations of cathepsin G (Fig. 7C). Cleavage within the RSL was seen when the mutant protein was assayed with cathepsin G concentrations of 60 nM or greater, but no SDS-stable complexes were formed. This strongly indicates that the P1 residue responsible for complex formation with cathepsin G is the phenylalanine at position 322. RSL cleavage of N321A/F322A/S323A and F322A in the absence of the proposed P1

phenylalanine at residue 322 probably occurs at the nearby phenylalanine, tyrosine, or methionine residues in the exposed RSL at amino acid residues 318, 319, 324, and 326 (Fig. 3).

A third mutant, T309R, was constructed which contains an arginine in place of threonine at the critical predicted P1 hinge region of SPI-1. It has been proposed that the presence of an arginine residue such as is seen in the hinge region of the noninhibitory serpins ovalbumin and angiotensinogen prevents RSL insertion into the serpin backbone, a step important for complex formation and the inhibitory activity of serpins (12, 16). ^{35}S -labeled T309R synthesized in the TNT system was assayed for complex formation with cathepsin G (Fig. 7D). As with the other mutant proteins, complex formation with cathepsin G did not occur. The inability of the T309R mutant

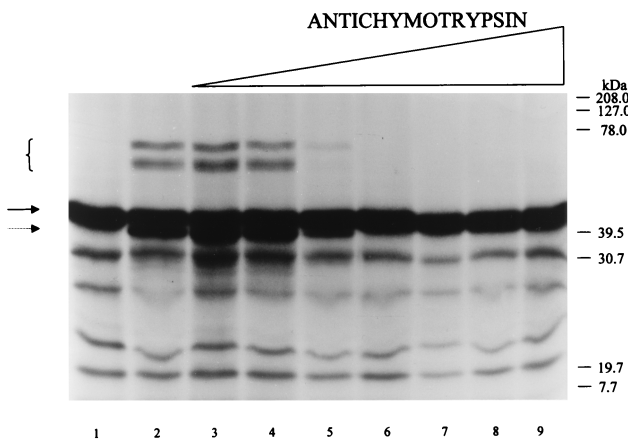


FIG. 5. Reaction of SPI-1 with cathepsin G in the presence of the competing serpin antichymotrypsin. ^{35}S -labeled SPI-1 prepared in the TNT system was incubated with buffer (lane 1) or with 200 nM cathepsin G in the absence (lane 2) or presence of 3-fold increasing concentrations of antichymotrypsin ranging from 20 nM (lane 3) to 20 μM (lane 9). Reactions were performed at 37°C for 90 min. Proteins were resolved on SDS-10% polyacrylamide gels, and radiolabeled proteins were visualized by autoradiography. Uncleaved SPI-1 is visible as a ~45-kDa band in lane 1 (solid arrow). SPI-1 cleaved within the RSL appears as a ~39.5-kDa band (dashed arrow), while higher-molecular-mass bands representing SDS-stable complexes with cathepsin G (brackets) are present in lanes 2 to 4.

containing an arginine at the P14 site to form a complex with cathepsin G suggests that strand insertion is necessary for complex formation to occur, consistent with the inhibitory mechanism of serpins.

Host range restriction of RPV SPI-1 site-directed mutants. Previous work has demonstrated that the RPV SPI-1 gene is necessary for viral growth in restrictive cell lines and that infection of restrictive cell lines with RPV SPI-1 deletion mutants results in some of the features of apoptosis (1, 3). Since we have been able to demonstrate that SPI-1 has serpin activity in vitro, we wanted to determine whether serpin function correlates with full host range.

The RPV Δ SPI-1 mutant described above was used to create recombinant viruses in which the three different SPI-1 site-

directed mutant genes discussed above were introduced into the viral genome replacing the *gpt* gene. The presence of each of the mutant genes was confirmed by PCR, sequencing, and immunoblot analysis (data not shown). These mutant viruses, designated RPV SPI-1 N321A/F322A/S323A, RPV SPI-1 F322A, and RPV SPI-1 T309R, each contained the mutant SPI-1 genes in place of the native SPI-1 gene and were regulated by the native SPI-1 gene promoter. Expression of the mutant genes therefore occurred at the appropriate time and at the same levels as for the wt gene during infection.

wt RPV, RPV Δ SPI-1, RPV SPI-1 N321A/F322A/S323A, RPV SPI-1 F322A, and RPV SPI-1 T309R were plaque on RK13, A549, and PK15 cells to determine the host range of the viral recombinants (Fig. 8). wt RPV was able to form plaques on all cell lines, while RPV Δ SPI-1 was unable to form plaques on the two restrictive A549 and PK15 cell lines, consistent with published results (1). The mutant viruses RPV SPI-1 N321A/F322A/S323A, RPV SPI-1 F322A, and RPV SPI-1 T309R were each able to form plaques on RK13 cells but were unable to do so on A549 or PK15 cells. The inability of the RPV SPI-1 site-directed mutants to form plaques on the cell lines restrictive for RPV Δ SPI-1 suggests that the mutations which inhibited the serpin function of SPI-1 (Fig. 7) also destroyed the ability of the virus to maintain a normal, full host range (Fig. 8).

Nuclear morphology of A549 cells infected with RPV SPI-1 site-directed mutants. We have demonstrated that RPV recombinants containing site-directed mutations of SPI-1 display the same reduced host range as the RPV SPI-1 deletion mutant did. We wanted to determine if the host range restriction of these recombinant viruses correlated with the apoptotic-like morphology observed in the nonpermissive cells infected with SPI-1 deletion mutants (3). A549 cells were mock infected or infected with wtRPV, RPV Δ SPI-1, RPV SPI-1 N321A/F322A/S323A, RPV SPI-1 F322A, or RPV SPI-1 T309R at an MOI of 10. At 18 h postinfection, cells were fixed, permeabilized, and stained with the fluorescent DNA-specific dye DAPI (Fig. 9). Unlike mock- or wtRPV-infected cells, nuclei from A549 cells infected with either of the three site-directed mutants displayed the chromatin condensation and nuclear invagination characteristic of apoptotic cells. Thus, the morphology observed in nonpermissive cells infected with any of the RPV

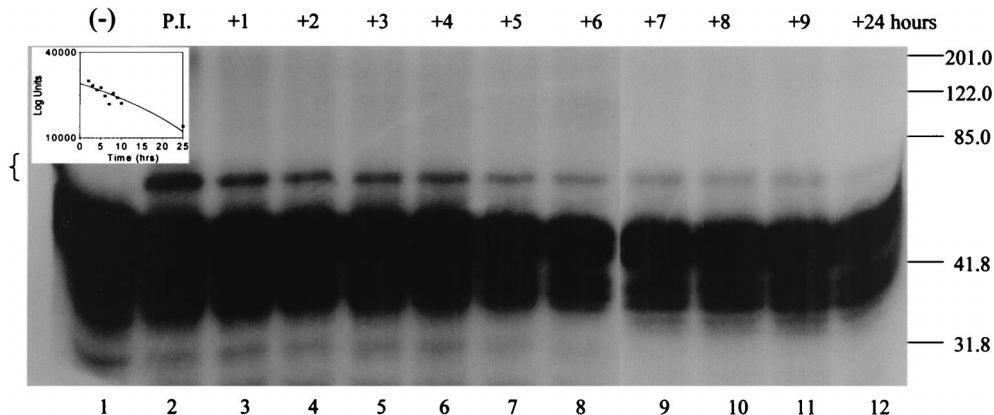


FIG. 6. Stability of the SPI-1-cathepsin G complex. ^{35}S -labeled SPI-1 prepared in the TNT system (lane 1) was preincubated in the presence of 200 nM cathepsin G for 60 min at 37°C (P.I., lane 2) to allow complex formation. Following the 1-h preincubation, antichymotrypsin was added in excess to a final concentration of 2 μM to quench any unreacted cathepsin G and the reaction mixture was incubated for another 24 h at 37°C. Samples were removed at 1 (lane 3), 2 (lane 4), 3 (lane 5), 4 (lane 6), 5 (lane 7), 6 (lane 8), 7 (lane 9), 8 (lane 10), 9 (lane 11), and 24 (lane 12) h after the addition of antichymotrypsin, and the proteins were resolved on an SDS-10% polyacrylamide gel. Radiolabeled proteins were visualized by autoradiography. High-molecular-mass bands representing the complex between SPI-1 and cathepsin G in lanes 3 to 12 of the gel were measured with a PhosphorImager. PhosphorImager measurements from three separate experiments were averaged and are expressed graphically in log units versus time (inset).

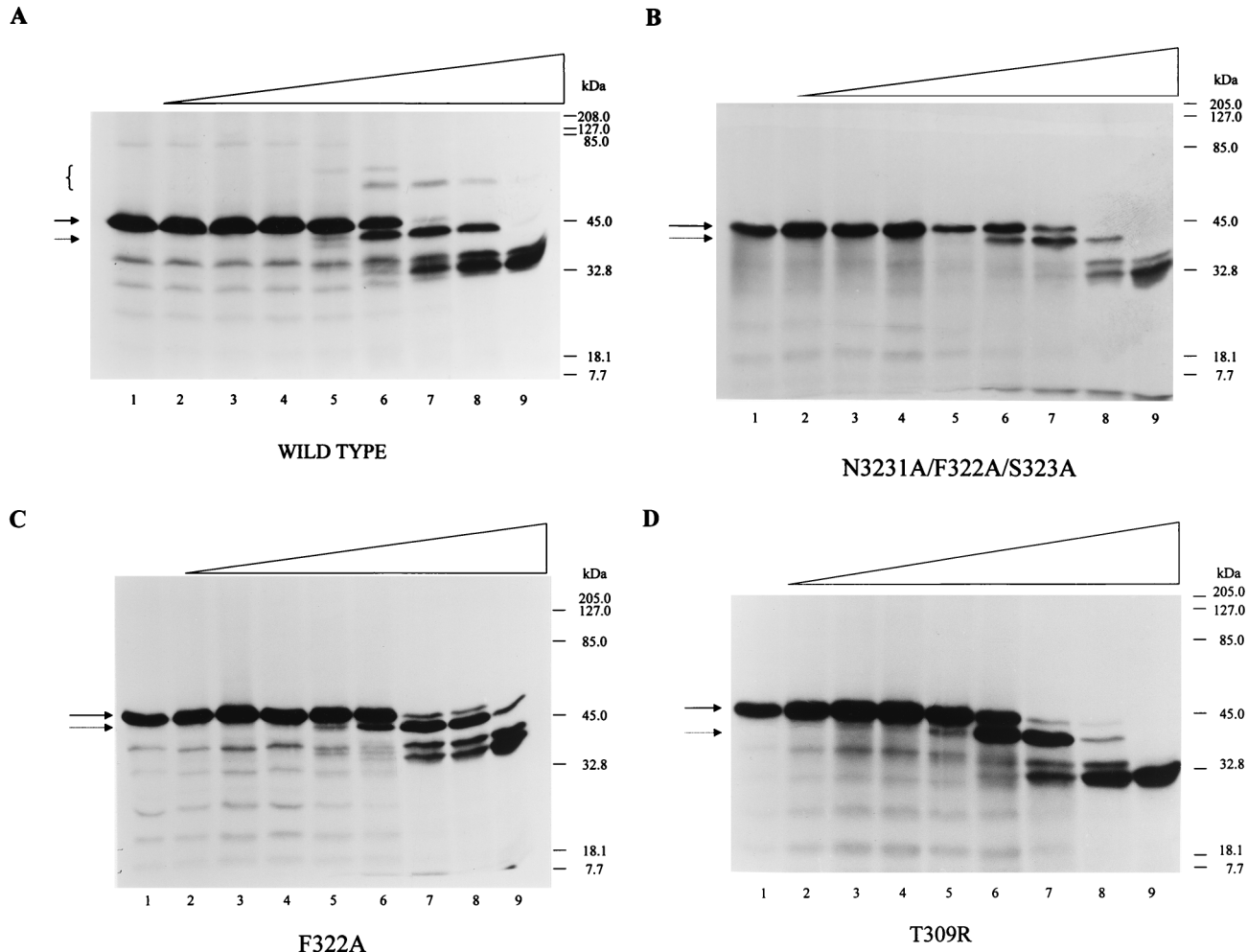


FIG. 7. Site-directed mutagenesis of the SPI-1 RSL and effect on complex formation. ^{35}S -labeled wt SPI-1 (A), N3231A/F322A/S323A (B), F322A (C), and T309R (D) were prepared in the TNT system and assayed alone (lanes 1) or with threefold-increasing concentrations of cathepsin G ranging from 2 nM (lanes 2) to 6 μM (lanes 9). Reaction mixtures were incubated at 37°C for 90 min. The proteins were separated on SDS-10% polyacrylamide gels, and radiolabeled proteins were visualized by autoradiography. High-molecular-mass complexes between wt SPI-1 and cathepsin G are indicated by brackets. Intact and cleaved forms of wt or mutant SPI-1 are designated by a solid arrow and a dashed arrow, respectively.

mutants containing a SPI-1 gene which has lost serpin-like activity correlates with loss of host range and the induction of the morphological features of apoptosis.

DISCUSSION

Previous studies have demonstrated that RPV SPI-1 mutants display a reduced host range and are unable to productively infect several cell lines, including PK15 and A549 cells (1). It was proposed that infection of these restrictive cell lines with RPV SPI-1 mutants induced apoptosis which degraded progeny virions prior to their release from the cell (3). Phenotypically, infection of A549 cells with RPV SPI-1 mutants results in the chromatin condensation and nuclear invagination typically observed in cells undergoing apoptosis (3). Surprisingly, this study demonstrates that several of the biochemical features which are normally observed in apoptotic cells are absent. We have observed neither cleavage of the death substrates PARP and lamin A (Fig. 2A and B) nor activation of terminal caspases in A549 cells infected with an RPV SPI-1 deletion mutant (Fig. 2C). There are two possible explanations for these results. The first is that despite the morphological

indications of apoptosis, cell death occurs through another mechanism. The second is that death occurs through a novel apoptotic pathway not involving caspase activation. It is becoming apparent that caspase-independent as well as caspase-dependent forms of apoptosis exist and that they are triggered by different mechanisms. Apoptosis has been demonstrated to occur in cells in the presence of z-VAD, a general inhibitor of all caspases, or the baculovirus p35 protein, which is an effective inhibitor of caspases 1, 3, 6, 7, 8, and 10 (5, 25, 45). Several other studies have shown that when apoptosis is induced in the presence of broad-range caspase inhibitors, membrane blebbing, chromatin condensation, and nuclear compaction are observed in the absence of concomitant nuclear fragmentation and DNA laddering, suggesting that caspases are responsible for some but not all of the hallmarks of apoptosis (20, 25, 44). The lack of caspase activation in A549 cells infected with RPVΔSPI-1 suggests that such a caspase-independent mechanism of apoptosis may in fact be taking place.

Poxvirus serpins have been shown to exhibit a spectrum of activities, and two which contain aspartic acid at the P1 positions (crmA and SERP2) have been implicated in the regulation of apoptosis (see references 22 and 42 for recent reviews).

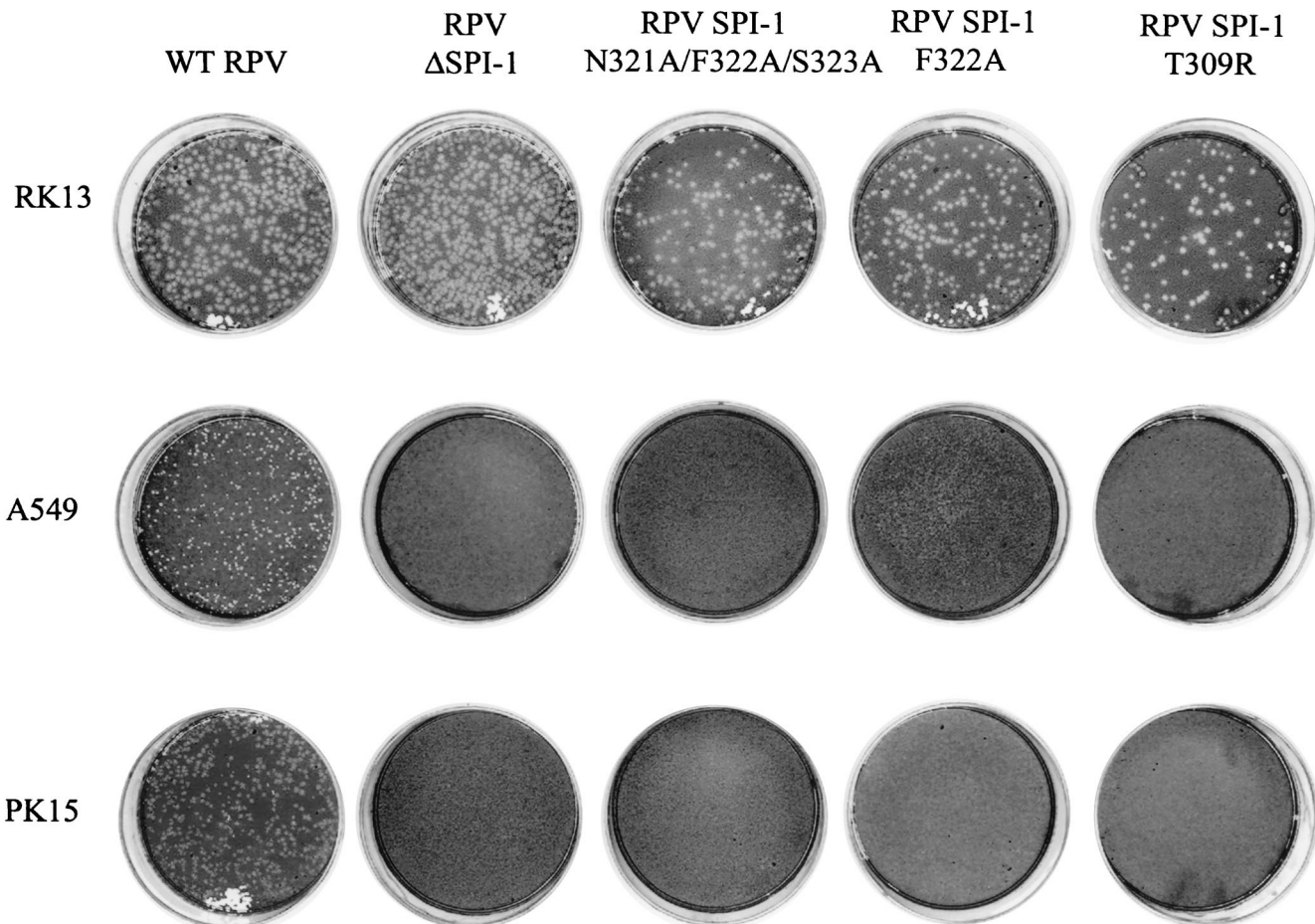


FIG. 8. Host range of wtRPV and RPV SPI-1 mutants. Plaque formation of wt RPV and RPV recombinants on RK13, A549, and PK15 cell lines is shown. The plaque assays were performed as described in Materials and Methods.

SPI-1 has 35% amino acid homology to all serpin family members and contains all of the conserved serpin motifs, including a small uncharged P14 residue necessary for RSL insertion and complex formation (Fig. 3). In this study, we showed that the SPI-1 protein from RPV complexes with cathepsin G (Fig. 4), indicating a probable function as a proteinase inhibitor. Complex formation occurs only with cathepsin G and not with the related chymotrypsin family members mast cell chymase and chymotrypsin (Fig. 4A) or with serine proteinases from other families (data not shown), indicating that the reaction between SPI-1 and cathepsin G is specific. Complex formation between SPI-1 and cathepsin G is prevented in the presence of antichymotrypsin (Fig. 5), an inhibitory serpin active against chymotrypsin family members, indicating that active cathepsin G is necessary for complex formation to occur and that SPI-1 and antichymotrypsin compete for the same active site of cathepsin G. Once formed, the complex between SPI-1 and cathepsin G is stable, with an estimated half-life of 22.5 h (Fig. 6). The ability to form a specific, long-lived, SDS-stable complex with cathepsin G is consistent with the ability of SPI-1 to inhibit enzyme activity. Furthermore, the ability of SPI-1 to form a complex with cathepsin G is destroyed when amino acids essential for serpin activity are mutated (Fig. 7). Both N321A/F322A/S323A and F322A contain mutations at the predicted P1 residue (amino acid 322) and are unable to form a complex with cathepsin G (Fig. 7B and C). Likewise, T309R, which

contains a charged arginine in place of threonine at the P14 position (Fig. 7D), is unable to complex with cathepsin G, suggesting that RSL insertion into the serpin backbone is necessary for complex formation to occur. These data suggest that SPI-1 acts as an inhibitory serpin with a P1 residue of phenylalanine and is able to form a specific, long-lived, SDS-stable complex with cathepsin G. We are attempting to purify SPI-1 protein in order to more fully prove direct inhibition of cathepsin G by SPI-1. Several attempts to purify active forms of SPI-1 variants containing different N-terminal affinity tags from bacteria or infected cells have been unsuccessful.

Cathepsin G is a 25-kDa serine proteinase found in the azurophil granules of neutrophils, monocytes, and mast cells, and it functions as a bactericidal protease, cleaving after phenylalanine, methionine, and leucine residues (6, 34, 36, 40). Cathepsin G released from activated neutrophils is able to promote lymphocyte activation (13, 46) and act as a chemoattractant for mononuclear cells and neutrophils (7), increasing inflammation at the site of an immune response. Cathepsin G has also been shown to enhance the cytotoxicity of T cells and natural killer (NK) cells by binding to the cells and activating them (47). The proteolytic activity of cathepsin G is necessary for each of these biological functions (47). Because the cell-mediated immune response is important in countering a poxvirus infection (4), it is interesting that poxviruses encode a gene product capable of targeting and inhibiting cathepsin G

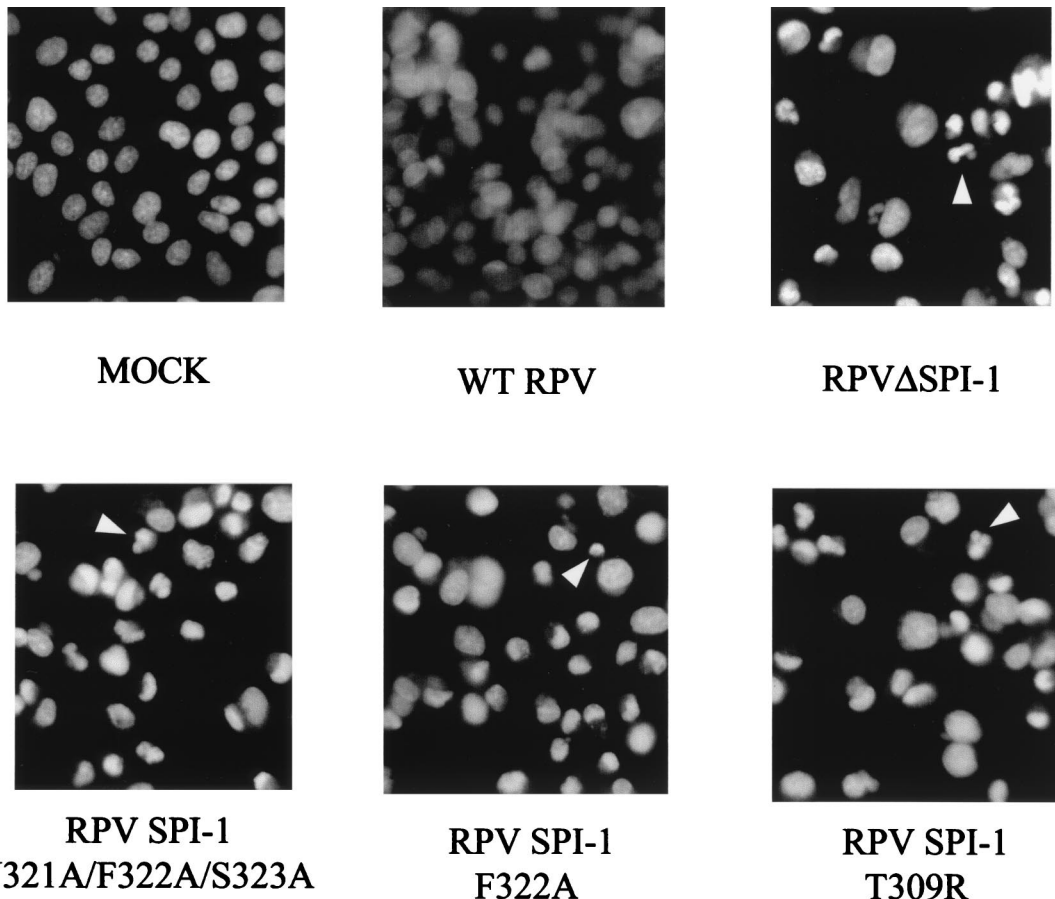


FIG. 9. DAPI staining of cells infected with wtRPV and RPV SPI-1 mutants. A549 cells were mock infected with medium alone or infected with wtRPV, RPVΔSPI-1, RPV SPI-1 N321A/F322A/S323A, RPV SPI-1 N322A, or RPV SPI-1 T309R at an MOI of 10. Cells were stained with DAPI 18 h after infection to display the cellular DNA and nuclear morphology. Arrowheads indicate condensed nuclei.

as a possible means of preventing inflammation and lymphocyte activation. While our model of cathepsin G inhibition by SPI-1 is based on in vitro analysis, in vivo experiments with wtRPV and RPV SPI-1 mutants should enable us to determine whether cathepsin G inactivation takes place during an infection.

The present study also demonstrates that the serpin activity of SPI-1 is required for virus growth in A549 human lung carcinoma and PK15 pig kidney cell lines. Mutant RPV bearing a single mutation at either the P1 or P14 sites of SPI-1 behaved like an RPV SPI-1 deletion mutant and was unable to grow in these restrictive cell lines (Fig. 8). These results imply that SPI-1 must inhibit a serine proteinase of chymotrypsin-like specificity to allow full host range. In contrast, site-directed mutagenesis of the serpin RSL of the related poxvirus serpin SPI-3 did not affect the ability of the protein to prevent cell fusion in infected cells (41), suggesting that the ability of SPI-1 to confer viral host range, unlike the ability of SPI-3 to prevent cell fusion, is related to serpin function.

The fact that the altered morphology of nonpermissive cells infected with RPV mutants which lack SPI-1 serpin activity is confined to the nuclei suggests that the serine proteinase target of SPI-1 in restrictive cells may function to regulate nuclear structure. While cathepsin G may be the natural target of SPI-1 in infected animals, it is unlikely to be the target protease in the infected tissue culture cells used in this study, since immunoblot analysis of RK13, PK15, and A549 cell extracts indicates

that cathepsin G is absent in these cells (data not shown). A Ca^{2+} -regulated serine proteinase with chymotryptic activity is associated with the nuclear scaffold (NS-associated protease) (8). Inhibition of the protease with AAPFcmk, a peptide inhibitor of chymotrypsin-like proteinases, has been shown to prevent lamin B1 breakdown and chromatin cleavage in nuclei incubated in the presence of apoptotic extracts (48, 49). Inhibition of the protease was also shown to prevent lamin B1 degradation in thymocytes and lamin degradation, histone H1 cleavage, and DNA fragmentation in thymocyte nuclei incubated with calcium, all of which could also be inhibited by overexpression of Bcl-2 (21). In light of the fact that RPV SPI-1 mutant infections of restrictive cells are characterized by chromatin condensation and nuclear invagination, SPI-1 inhibition of the NS-associated protease is an attractive hypothesis and predicts that SPI-1 may localize to the nucleus. This model is currently being tested.

ACKNOWLEDGMENTS

This work was funded by grant AI-15722 from the National Institutes of Health. K.B.M. is supported by NIH training grant T32-AI-07110, and P.C.T. is supported by grant 9701732 from the American Heart Association Florida affiliate.

We thank Norman Schechter for the generous gift of mast cell chymase and Harvey Rubin for discussions. The PARP cDNA clone was provided by B. Burke, and the lamin A clone was a gift from Alexander Burkle. We thank Michael Duke for excellent technical

assistance, M. Teresa Baquero for construction of the pALTER-Ex-1 (PARP) construct, and Traci Ness for critical reading of the manuscript.

REFERENCES

- Ali, A. N., P. C. Turner, M. A. Brooks, and R. W. Moyer. 1994. The SPI-1 gene of rabbitpox virus determines host range and is required for hemorrhagic pock formation. *Virology* **202**:306–314.
- Boyle, D. B., and B. E. Coupar. 1988. A dominant selectable marker for the construction of recombinant poxviruses. *Gene* **65**:123–128.
- Brooks, M. A., A. N. Ali, P. C. Turner, and R. W. Moyer. 1995. A rabbitpox virus serpin gene controls host range by inhibiting apoptosis in restrictive cells. *J. Virol.* **69**:7688–7698.
- Buller, R. M., and G. J. Palumbo. 1991. Poxvirus pathogenesis. *Microbiol. Rev.* **55**:80–122.
- Bump, N. J., M. Hackett, M. Hugunin, S. Seshagiri, K. Brady, P. Chen, C. Ferenz, S. Franklin, T. Ghayur, L. P. P. Licari, J. Mankovich, L. Shi, A. H. Greenberg, L. K. Miller, and W. W. Wong. 1995. Inhibition of the ICE family proteases by baculovirus antiapoptotic protein p35. *Science* **269**:1885–1888.
- Campbell, E. J., E. K. Silverman, and M. A. Campbell. 1989. Elastase and cathepsin G of human monocytes. Quantification of cellular content, release in response to stimuli, and heterogeneity in elastase-mediated proteolytic activity. *J. Immunol.* **143**:2961–2968.
- Chertov, O., H. Ueda, L. L. Xu, K. Tani, W. J. Murphy, J. M. Wang, O. M. Howard, T. J. Sayers, and J. J. Oppenheim. 1997. Identification of human neutrophil-derived cathepsin G and azurocidin/CAP37 as chemoattractants for mononuclear cells and neutrophils. *J. Exp. Med.* **186**:739–747.
- Clawson, G. A., L. L. Norbeck, C. L. Hatem, C. Rhodes, P. Amiri, J. H. McKerrow, S. R. Patierno, and G. Fiskum. 1992. Ca(2+)-regulated serine protease associated with the nuclear scaffold. *Cell Growth Differ.* **3**:827–838.
- Enari, M., H. Hug, and S. Nagata. 1995. Involvement of an ICE-like protease in Fas-mediated apoptosis. *Nature* **375**:78–81.
- Falkner, F. G., and B. Moss. 1988. *Escherichia coli gpt* gene provides dominant selection for vaccinia virus open reading frame expression vectors. *J. Virol.* **62**:1849–1854.
- Gagliardini, V., P. A. Fernandez, R. K. Lee, H. C. Drexler, R. J. Rotello, M. C. Fishman, and J. Yuan. 1994. Prevention of vertebrate neuronal death by the crmA gene. *Science* **263**:826–828. (Erratum, **264**:1388, 1994.)
- Gettins, P., P. A. Patston, and M. Schapira. 1993. The role of conformational change in serpin structure and function. *Bioessays* **15**:461–467.
- Hase-Yamazaki, T., and Y. Aoki. 1995. Stimulation of human lymphocytes by cathepsin G. *Cell. Immunol.* **160**:24–32.
- Huber, R., and R. W. Carrell. 1989. Implications of the three-dimensional structure of alpha 1-antitrypsin for structure and function of serpins. *Biochemistry* **28**:8951–8966.
- Lawrence, D. A., D. Ginsburg, D. E. Day, M. B. Berkenpas, I. M. Verhamme, J. Kvassman, and J. D. Shore. 1995. Serpin-protease complexes are trapped as stable acyl-enzyme intermediates. *J. Biol. Chem.* **270**:25309–25312.
- Lawrence, D. A., S. T. Olson, S. Palaniappan, and D. Ginsburg. 1994. Serpin reactive center loop mobility is required for inhibitor function but not for enzyme recognition. *J. Biol. Chem.* **269**:27657–27662.
- Los, M., M. Van de Craen, L. C. Penning, H. Schenk, M. Westendorp, P. A. Baeuerle, W. Droege, P. H. Krammer, W. Fiers, and K. Schulze-Osthoff. 1995. Requirement of an ICE/CED-3 protease for Fas/APO-1-mediated apoptosis. *Nature* **375**:81–83.
- Macen, J., A. Takahashi, K. B. Moon, R. Nathaniel, P. C. Turner, and R. W. Moyer. 1998. Activation of caspases in pig kidney cells infected with wild-type and CrmA/SPI-2 mutants of cowpox and rabbitpox viruses. *J. Virol.* **72**:3524–3533.
- Macen, J. L., R. S. Garner, P. Y. Musy, M. A. Brooks, P. C. Turner, R. W. Moyer, G. McFadden, and R. C. Bleackley. 1996. Differential inhibition of the Fas- and granule-mediated cytolysis pathways by the orthopoxvirus cytokine response modifier A/SPI-2 and SPI-1 protein. *Proc. Natl. Acad. Sci. USA* **93**:9108–9113.
- McCarthy, N. J., M. K. Whyte, C. S. Gilbert, and G. I. Evan. 1997. Inhibition of Ced-3/ICE-related proteases does not prevent cell death induced by oncogenes, DNA damage, or the Bcl-2 homologue Bak. *J. Cell Biol.* **136**:215–227.
- McConkey, D. J. 1996. Calcium-dependent, interleukin 1-converting enzyme inhibitor-insensitive degradation of lamin B1 and DNA fragmentation in isolated thymocyte nuclei. *J. Biol. Chem.* **271**:22398–22406.
- McFadden, G., and M. Barry. 1998. How poxviruses control apoptosis. *Semin. Virol.* **8**:429–442.
- Miura, M., H. Zhu, R. Rotello, E. A. Hartwig, and J. Yuan. 1993. Induction of Apoptosis in fibroblasts by IL-1 β converting enzyme, a mammalian homolog of the *C. elegans* cell death gene CED-3. *Cell* **75**:653–660.
- Nicholson, D. W., and N. A. Thornberry. 1997. Caspases: killer proteases. *Trends Biochem. Sci.* **22**:299–306.
- Okuno, S., S. Shimizu, T. Ito, M. Nomura, E. Hamada, Y. Tsujimoto, and H. Matsuda. 1998. Bcl-2 prevents caspase-independent cell death. *J. Biol. Chem.* **273**:34272–34277.
- Owen, M. C., S. O. Brennan, J. H. Lewis, and R. W. Carrell. 1983. Mutation of antitrypsin to antithrombin alpha 1-antitrypsin Pittsburgh (358 Met leads to Arg), a fatal bleeding disorder. *N. Engl. J. Med.* **309**:694–698.
- Patston, P. A. 1995. Studies on inhibition of neutrophil cathepsin G by alpha 1-antichymotrypsin. *Inflammation* **19**:75–81.
- Potempa, J., E. Korzus, and J. Travis. 1994. The serpin superfamily of proteinase inhibitors: structure, function, and regulation. *J. Biol. Chem.* **269**:15957–15960.
- Quan, L. T., A. Caputo, R. C. Bleackley, D. J. Pickup, and G. S. Salvesen. 1995. Granzyme B is inhibited by the cowpox virus serpin cytokine response modifier A. *J. Biol. Chem.* **270**:10377–10379.
- Ray, C. A., R. A. Black, S. R. Kronheim, T. A. Greenstreet, P. R. Sleath, G. S. Salvesen, and D. J. Pickup. 1992. Viral inhibition of inflammation: cowpox virus encodes an inhibitor of the interleukin-1 beta converting enzyme. *Cell* **69**:597–604.
- Ray, C. A., and D. J. Pickup. 1996. The mode of death of pig kidney cells infected with cowpox virus is governed by the expression of the crmA gene. *Virology* **217**:384–391.
- Razvi, E. S., and R. M. Welsh. 1995. Apoptosis in viral infections. *Adv. Virus Res.* **45**:1–60.
- Rubin, H. 1996. Serine protease inhibitors (SERPINS): where mechanism meets medicine. *Nat. Med.* **2**:632–633.
- Salvesen, G., D. Farley, J. Shuman, A. Przybyla, C. Reilly, and J. Travis. 1987. Molecular cloning of human cathepsin G: structural similarity to mast cell and cytotoxic T lymphocyte proteinases. *Biochemistry* **26**:2289–2293.
- Schechter, N. M., L. M. Jordan, A. M. James, B. S. Cooperman, Z. M. Wang, and H. Rubin. 1993. Reaction of human chymase with reactive site variants of alpha 1-antichymotrypsin. Modulation of inhibitor versus substrate properties. *J. Biol. Chem.* **268**:23626–23633.
- Schechter, N. M., Z. M. Wang, R. W. Blacher, S. R. Lessin, G. S. Lazarus, and H. Rubin. 1994. Determination of the primary structures of human skin chymase and cathepsin G from cutaneous mast cells of urticaria pigmentosa lesions. *J. Immunol.* **152**:4062–4069.
- Stein, P. E., and R. W. Carrell. 1995. What do dysfunctional serpins tell us about molecular mobility and disease. *Nat. Struct. Biol.* **2**:96–113.
- Takahashi, A., E. S. Alnemri, Y. A. Lazebnik, T. Fernandes-Alnemri, G. Litwack, R. D. Moir, R. D. Goldman, G. G. Poirier, S. H. Kaufmann, and W. C. Earnshaw. 1996. Cleavage of lamin A by Mch2 α but not by CPP32: multiple interleukin 1 β converting enzyme-related proteases with distinct substrate recognition properties are active in apoptosis. *Proc. Natl. Acad. Sci. USA* **93**:8395–8400.
- Tewari, M., and V. M. Dixit. 1995. Fas- and tumor necrosis factor-induced apoptosis is inhibited by the poxvirus crmA gene product. *J. Biol. Chem.* **270**:3255–3260.
- Travis, J. 1988. Structure, function, and control of neutrophil proteinases. *Am. J. Med.* **84**:37–42.
- Turner, P. C., and R. W. Moyer. 1992. An orthopoxvirus serpinlike gene controls the ability of infected cells to fuse. *J. Virol.* **66**:2076–2085.
- Turner, P. C., and R. W. Moyer. 1998. Control of apoptosis by poxviruses. *Semin. Virol.* **9**:453–469.
- Virgin, H. W., P. Latreille, P. Wamsley, K. Hallsworth, K. E. Week, A. J. Dalcanto, S. H. Speck, H. W. Virgin IV, and A. J. Dal Canto. 1997. Complete sequence and genomic analysis of murine gammaherpesvirus 68. *J. Virol.* **71**:5894–5904.
- Xiang, J., D. T. Chao, and S. J. Korsmeyer. 1996. BAX-induced cell death may not require interleukin 1 beta-converting enzyme-like proteases. *Proc. Natl. Acad. Sci. USA* **93**:14559–14563.
- Xue, D., and H. R. Horvitz. 1995. Inhibition of the *Caenorhabditis elegans* cell-death protease CED-3 by a CED-3 cleavage site in baculovirus p35 protein. *Nature* **377**:248–251.
- Yamazaki, T., and Y. Aoki. 1997. Cathepsin G binds to human lymphocytes. *J. Leukoc. Biol.* **61**:73–79.
- Yamazaki, T., and Y. Aoki. 1998. Cathepsin G enhances human natural killer cytotoxicity. *Immunology* **93**:115–121.
- Zhivotovsky, B., A. Gahm, M. Ankarcrona, P. Nicotera, and S. Orrenius. 1995. Multiple proteases are involved in thymocyte apoptosis. *Exp. Cell Res.* **221**:404–412.
- Zhivotovsky, B., A. Gahm, and S. Orrenius. 1997. Two different proteases are involved in the proteolysis of lamin during apoptosis. *Biochem. Biophys. Res. Commun.* **233**:96–101.
- Zhou, Q., S. Snipas, K. Orth, M. Muzio, V. M. Dixit, and G. S. Salvesen. 1997. Target protease specificity of the viral serpin CrmA—analysis of five caspases. *J. Biol. Chem.* **272**:7797–7800.